The essential role of *Dnmt1* in gametogenesis in the large milkweed bug *Oncopeltus fasciatus*

Joshua T. Washington[1], Katelyn R. Cavender[1], Ashley U. Amukamara[1], Elizabeth C. McKinney[1], Robert J. Schmitz[2], Patricia J. Moore[1,*]

[1] Department of Entomology, University of Georgia

[2] Department of Genetics, University of Georgia

*Patricia J. Moore, 413 Biological Sciences Building, Department of Entomology, University of Georgia, Athens, GA, 30602; (706) 542-0169

Email: pjmoore@uga.edu

Patricia J. Moore: https://orcid.org/0000-0001-9802-7217

Robert J. Schmitz: https://orcid.org/0000-0001-7538-6663

Keywords

DNA methylation, epigenetics, *Dnmt1*, spermatogenesis, germ cells, *Oncopeltus fasciatu*

Abstract

Given the importance of DNA methylation in protection of the genome against transposable elements and transcriptional regulation in other taxonomic groups, the diversity in both levels and patterns of DNA methylation in the insects raises questions about its function and evolution. We show that the maintenance DNA methyltransferase, DNMT1, affects meiosis and is essential to fertility in milkweed bugs, *Oncopeltus fasciatus*, while DNA methylation is not required in somatic cells. Our results support the hypothesis that *Dnmt1* is required for the transition of germ cells to gametes in *O. fasciatus* and that this function is conserved in male and female gametogenesis. They further suggest that DNMT1 has a function independent of DNA methylation in germ cells. Our results raise the question of how a gene so critical in fitness across multiple insect species can have diverged widely across the insect tree of life.

13 **Introduction**

14 Despite the apparent ubiquity of DNA methylation across the eukaryotic tree of life (Schmitz et
15 al. 2019, Lewis et al. 2020), in the insects there is considerable variation both in the presence and
16 extent of DNA methylation and even the presence and number of the DNA methyltransferases
17 (Bewick et al. 2016, Lyko 2018, Glastad et al. 2019). Thus, the functional role of DNA
18 methylation and its associated DNA methyltransferases in the insects is unclear. While some
19 studies have associated levels of methylation with gene expression, most studies in the insects
20 find no functional association (Bewick et al. 2016, Glastad et al. 2019).

21 One role emerging from knockdown and silencing studies across several insect species is that
22 *Dnmt1* is required for oogenesis (Schulz et al. 2018, Bewick et al. 2019, Gegner et al. 2019,
23 Amukamara et al. 2020). For example, *Dnmt1* is required for maintenance of DNA methylation
24 following cell division in the milkweed bug, *Oncopeltus fasciatus* (Bewick et al. 2019,
25 Amukamara et al. 2020), the downregulation of *Dnmt1* using RNAi results in a reduction in
26 methylation and also the cessation of oogenesis. However, it is unclear whether the effect on
27 oogenesis is mediated by the reduction in DNA methylation (Amukamara et al. 2020). While the
28 expected reduction in DNA methylation is seen throughout the organism following *Dnmt1*
29 knockdown, the only phenotypic consequence is to the germ cells. Evidence from other species
30 supports a function independent of DNA methylation. *Dnmt1* is also essential to egg production
31 in *T. castaneum* (Schulz et al. 2018), a beetle that has no DNA methylation at all (Zemach et al.
32 2010). This suggests that *Dnmt1* can have a function specific to germ cells in insects that is
33 independent of its function in maintaining DNA methylation. This led us to hypothesize that
34 *Dnmt1* plays a role in meiosis in insects (Amukamara et al. 2020).

35 In this study, we tested the hypothesis that *Dnmt1* is essential to gametogenesis in *O. fasciatus*.
36 Furthermore, if *Dnmt1* has a role in gametogenesis, including meiosis, it should be conserved
37 across the sexes. Testing the function of *Dnmt1* in males allows us to capitalize on the well-
38 characterized process of spermatogenesis in *O. fasciatus*, specifically (illustrated in Figure 1;
39 Economopoulos & Gordon 1971), and the conserved features of insect spermatogenesis,
40 generally (Dallai 2014). In *O. fasciatus,* as in many insects, there are two points in development
41 where meiosis can occur. The first stage where meiosis will occur is during the larval stages.
42 Testis development and spermatogenesis is initiated during larval development in *O. fasciatus*
43 (Economopoulos & Gordon 1971). During the first three instars the testes consist of seven
44 globular follicles that will develop into the testis tubules (Schmidt et al. 2002). Meiosis is
45 initiated in the 4th instar, and by the end of the 4th instar, cysts containing spermatids are present.
46 Differentiation of the spermatids commences in the 5th instar, and males emerge with up to
47 250,000 spermatids that continue to differentiate during sexual maturation. Thus, we can target
48 the developmental time point at which meiosis occurs. In addition, *O. fasciatus* males can
49 produce gametes throughout their adult lives and therefore meiosis can occur in the adult testis.
50 If *Dnmt1* is required for meiosis and gametogenesis we predicted that it will be required both
51 during larval development and as adult males replenish sperm stores following mating. We
52 therefore compared the testis phenotypes of adults developing from nymphs in which *Dnmt1*
53 expression was downregulated either before or after the major wave of meiosis that occurs in
54 testis development (Economopoulos & Gordon 1971, Schmidt et al. 2002, Ewen-Campen et al
55 2013). We also treated sexually mature adults, and examined fertility in males following sperm
56 depletion, testing for the ability of knockdown males to replenish sperm stores following
57 multiple matings. Our results demonstrated that expression of *Dnmt1* is required for the

58 development of sperm both during larval and adult spermatogenesis and that the impact of
59 *Dnmt1* knockdown was greatest if it occurred prior to the onset of meiotic divisions in the
60 developing testes. These results establish that *Dnmt1* plays a critical conserved function across
61 the sexes during gametogenesis in *O. fasciatus* and that it is required for germ cell development.

62 **Results**

63 **The pattern of *Dnmt1* expression during testis development and across tissues suggests a**
64 **role in spermatogenesis.**

65 We measured *Dnmt1* expression during larval development and sexual maturation. Our
66 prediction was that if *Dnmt1* is required during gametogenesis, particularly meiosis, then its
67 expression should mirror those of two genes known to be involved in germ cell development,
68 *Boule* and *Vasa* (Shah et al. 2010, Yajima & Wessel 2011). Thus, we predicted that *Dnmt1*
69 expression would be highest during the stages when gametogenesis is occurring. As predicted,
70 testis-specific expression of *Dnmt1* is highest during the 4th and 5th instars of development
71 (Figure 2A; ANOVA, $F = 27.426$, d.f. = 3, 38, $p < 0.001$), stages when meiosis and
72 spermatogenesis is most active (Economopoulos & Gordon 1971). The expression is lowest in
73 virgin adult males. This expression pattern mirrored that observed for *Boule*, a gene with a well-
74 characterized role in meiosis (Figure 2B; ANOVA, $F = 36.346$, d.f. = 3, 38, $p < 0.001$). *Dnmt1*
75 expression pattern was also similar to *Vasa*, a highly conserved marker of the germline (Figure
76 2C; ANOVA, $F = 20.444$, d.f. = 3, 38, $p < 0.001$). While *Dnmt1* is expressed across all adult
77 tissues, as would be expected given its role in maintenance of DNA methylation, expression is
78 highest in testes compared to gut, head, and muscle tissue (Figure S2; ANOVA, $F = 67.311$, d.f.
79 = 3, 36, $p < 0.001$), also suggesting a special role during gametogenesis.

80 ***Dnmt1* knockdown reduced levels of DNA methylation in the testis genome**.

81 To confirm the effectiveness of our RNAi treatment, we measured expression of *Dnmt1* in a
82 subset of ds-RED and ds-*Dnmt1* injected males (Figure 3). Quantitative PCR demonstrated
83 reduced levels of *Dnmt1* mRNA in ds-*Dnmt1* injected males compared to ds-RED injected males
84 in both 3rd instar (ANOVA; $F = 83.126$, d.f. = 1, 31, $p < 0.001$) and 5th instar (ANOVA; $F =$
85 49.793, d.f. = 1, 22, $p < 0.001$) treated males 6 to 10 days following injection with dsRNA.
86 Treatment of males with ds-*Dnmt1* had the predicted effect on *Dnmt1* expression. We performed
87 whole genome bisulfite sequencing to evaluate the impact of the ds-*Dnmt1* on DNA methylation
88 genome wide. The reduction in expression of *Dnmt1* in the RNAi individuals had the expected
89 phenotypic effect on DNA methylation with a reduction of genome methylation in the testes for
90 ds-*Dnmt1* treated males, but not control males (Supplementary materials, Figure S2). Genomic
91 DNA from the testes of control treated males had approximately 12.5% CpG methylation
92 regardless of stage they were treated. Knockdown of *Dnmt1* at the earlier stage of development
93 led to a greater percentage reduction of methylation. Treatment with ds-*Dnmt1* at the 5th instar
94 reduced the percent CpG methylation from around 12.5% to around 5%. Treatment with ds-
95 *Dnmt1* at the 3rd instar reduced the level of methylation even further, to around 2%, as predicted
96 given the greater numbers of cell divisions that were expected between treatment and sampling
97 between these two treatments.

98 ***Dnmt1* knockdown affected testis size and structure.**

99 Knockdown of *Dnmt1* prior to meiosis, in the 3rd instar stage, had a significant effect on testis
100 size in virgin males, while knockdown of *Dnmt1* during the developmental stage after which
101 meiosis is initiated, the 5th instar stage, had no effect on testis size (Figure 4; ANOVA, $F =$
102 20.360, d.f. = 4, 58, $p < 0.001$) compared to either uninjected controls or ds-RED treated males.

103 Knockdown of *Dnmt1* prior to meiosis affected testis tubules to a greater extent than knockdown
104 following the initiation of meiosis during larval testis development (Figure 5). Control males
105 injected in the 3rd or 5th instar stage of development showed the expected structure of the testis
106 tubule (Figure 5A and C). At the anterior end of the testis tubule, spermatogonia and primary
107 spermatocytes had the characteristic nuclear structure and there was clear evidence of mitotic
108 division within the spermatogonia (Figure 5C, arrowhead), using α-phosphohistone H3 (pHH3)
109 to stain for chromosome condensation in preparation for mitosis and meiosis. We also observed
110 α-pHH3 staining in spermatocysts at the border between primary and secondary spermatocytes
111 in the control testis tubules in both 3rd and 5th instar treated males. Following this band of
112 relatively synchronous meiotic activity, the posterior testis tubule showed spermatids and
113 developing spermatozoa as they matured. We confirmed the use of this band of α-pHH3 stained
114 spermatocysts as a landmark of meiosis using knockdown of Boule (Supplementary materials,
115 Figure S3).

116 The structure of the testis tubules of males treated with ds-*Dnmt1* in the 3rd instar was highly
117 disrupted and both the anterior and posterior testis tubule was affected (Figure 5B). There were
118 fewer spermatocysts in both the region of spermatogonia and primary spermatocytes. While
119 there were occasional α-pHH3 positive nuclei, these were not well organized into spermatocysts
120 and were spread throughout the testis tubule rather than organized at the junction between
121 primary and secondary spermatocytes. There was evidence of mitotic activity in the
122 spermatogonia (Figure 5B arrowhead), although these were less frequent in ds-*Dnmt1* treated
123 males than control males. The testis tubules of males treated with ds-*Dnmt1* in the 5th instar stage
124 of development had a structure much more similar to control males (Figure 5D). Mitotic activity
125 was apparent in the spermatogonia (Figure 5D arrowhead) and most testis tubules had evidence

126 of mature sperm and α-pHH3 stained spermatocysts at the junction between primary and
127 secondary spermatocytes (Figure 5D arrow). Unorganized spermatocysts below this junction
128 were frequently observed, however, and ds-*Dnmt1* males treated at the 5th instar had variable
129 phenotypes posterior to the primary spermatocytes, presumably depending on when treatment
130 occurred following the wave of meiosis along the testis tubule axis.

131 ***Dnmt1* knockdown in adult males prevented replenishment of sperm stores**

132 Downregulating *Dnmt1* expression in adult males resulted in a loss of fecundity over time. The
133 third and final females mated to ds-*Dnmt1* treated males ran out of sperm to fertilize eggs more
134 rapidly than those mated to control males. Clutches of eggs laid by females mated to ds-*Dnmt1*
135 treated males were not fertilized and failed to hatch at an earlier collection day than those laid by
136 females mated to control males (Figure 6; Wilcoxon $\chi^2 = 13.978$, d. f. = 1, $p < 0.001$).

137 The loss of fertility in males was associated with smaller testis size. Males treated with ds-*Dnmt1*
138 at seven days post-emergence and then allowed to mate for three weeks prior to dissection had
139 statistically significantly smaller testis area than the testes of control males after the same mating
140 treatment (ANOVA, F = 29.084, d.f. = 1, 51, $p < 0.001$; Supplementary materials, Figure S4).
141 The smaller testis area of ds-*Dnmt1* treated adult males was associated with a breakdown in testis
142 tubule structure and the loss of sperm from the testis tubules (Figure 7). In control males, three
143 weeks post injection the regions of spermatogenesis were recognizable. Small spermatocysts
144 with spermatogonia undergoing mitotic divisions were observable at the anterior tip of the testis
145 tubule (Figure 7A and B). Posterior to the spermatogonia were the primary spermatocytes with
146 more diffuse nuclear structure. We often observed the band of α-pHH3 positive spermatocysts
147 that indicated the first meiotic division to form the secondary spermatocytes. At the most
148 posterior end of the testis tubule the spermatids developed into spermatozoa. Three weeks after

149 *Dnmt1* knockdown testis tubule structure is significantly disrupted. There appeared to be fewer
150 spermatogonia and those that remained had a more condensed nuclear structure than in the testis
151 tubules of control males (Figure 7C and D). The most noticable effect was seen in the region
152 containing the spermatocytes. There were few primary spermatocytes in the testis tubule and α-
153 pHH3 positively stained spermatocysts were rarely observed, indicating few spermatocysts
154 undergoing meiosis.

155 **Discussion**

156 The function of DNA methylation and the DNA methylation enzymes across the insect tree of
157 life has been widely debated, particularly in light of the extreme variation in presence of this
158 chromatin modification and the diversification of the enzymatic toolkit required to methylate
159 DNA *de novo* and maintain DNA methylation patterns (Bewick et al. 2016, Lyko 2018, Lewis et
160 al. 2020). This evolutionary pattern is particularly intriguing given that in two species on
161 divergent branches of the insect phylogeny the maintenance methyltransferase DNMT1 is
162 essential to gametogenesis, and thus is tightly tied to fitness, even in a species where DNA
163 methylation itself is absent (Schulz et al. 2018). While functional studies have not been done in
164 other species, a summary of expression studies on the DNA methyltransferases across a diversity
165 of insects suggest that these enzymes could be involved in gametogenesis across a number of
166 species, ranging from fire ants, *Solenopsis invicta* (Kay et al. 2018), to jewel wasps, N*asonia*
167 *vitripennis* (Zwier et al. 2012), to migratory locusts, *Locusta migratoria* (Robinson et al. 2016),
168 and the brown plant hopper, *Nilaparvata lugens* (Zhang et al. 2015). Here we showed that *Dnmt1*
169 expression affects germ cell development. The effect of downregulating *Dnmt1* in males, as in
170 females (Amukamara et al. 2020), was specific to the germ cells. The downregulation of *Dnmt1*
171 did result in reduction of DNA methylation, but there were no obvious morphological impacts to

172 the RNAi-treated individuals. Our results show that the function of *Dnmt1* in germ cells is
173 conserved across the sexes within a species, and other results document that *Dnmt1* expression is
174 required for oogenesis among species. This raises a conundrum when we look across the insect
175 tree of life. How can a gene required for such a fundamental fitness activity in examples from
176 such a diverse group of insects also be so evolutionarily labile? This suggests that the function
177 *Dnmt1* in germ cell development is easily lost or replaced.

178 ***Dnmt1* knockdown causes inhibition of spermatogenesis consistent with a role in meiosis**

179 If our hypothesis on the role of *Dnmt1* in meiosis is correct, then spermatogenesis should be
180 affected by *Dnmt1* expression as well as oogenesis, as it is a shared process across
181 gametogenesis during sexual reproduction. In the testes *O. fasciatus* males, we observed both
182 spermatogonia and primary spermatocytes that stain positively for phosphorylation of the serine
183 10 residue of histone protein H3. While the pattern of histone H3 phosphorylation across meiosis
184 has not been specifically studied in *O. fasciatus*, phosphorylation of the serine 10 is typically
185 associated with chromosome condensation during meiosis (Hans and Dimitrov 2001) and mitosis
186 (Prigent and Dimitrov 2003). Moreover, the pattern of α-pHH3 staining along the axis of the
187 testis tubule is consistent with this histone modification occurring in both mitosis and meiosis.
188 We observed α-pHH3 positive cells both within spermatocysts containing the mitotically
189 dividing spermatogonia and also at the boundary between primary and secondary spermatocytes.
190 We have confirmed this landmark using *Boule* knockdown males. In *Drosophila*, *Boule* is
191 required for progression of spermatocytes through meiosis. Germ cells lacking functional *Boule*
192 become arrested at meiotic prophase (Eberhart et al. 1996). In the testes of *O. fasciatus* males
193 treated with ds-*Boule*, the affected cells were all posterior to the band of synchronous α-pHH3
194 positive spermatocytes. Thus, α-pHH3 staining provided a landmark for entry into meiosis.

195 We did not see the band of α-pHH3 positive spermatocysts at the border between primary and
196 secondary spermatocytes in the *Dnmt1* knockdown males treated at the 3rd instar stage of
197 development. This could be interpreted as the primary spermatocytes have not initiated
198 chromosome condensation. However, we did observe individual α-pHH3 positive nuclei in the
199 posterior testis tubule. So there could have been arrest after chromatin condensation with a
200 breakdown in spermatocyst structure. Interestingly, the testis phenotype of our *Dnmt1*
201 knockdown males resembled the phenotypic effect of *Vasa* knockdown reported by Ewen
202 Campen et al. 2013. *Vasa* RNAi results in defects in cyst integrity and Ewen Campen et al.
203 (2013) propose that *Vasa* plays a specific role in the onset or synchrony of meiosis. *Vasa* has also
204 been proposed to be required for the correct progression through meiosis in mice (Tanaka et al.
205 2000) and humans (Medrano et al. 2012). Thus, the phenotypic similarity between *Dnmt1*
206 knockdown and *Vasa* knockdown testes in *O. faciatus* support the hypothesis that *Dnmt1* may be
207 required for the successful initiation and completion of meiosis in spermatocytes. More work
208 remains to determine exactly what stage of sperm development is impacted by the decrease in
209 *Dnmt1* expression.

210 The phenotype of knockdown of *Dnmt1* is exacerbated when knockdown occurs prior to the
211 stage of testis development when meiosis occurs. This result is consistent with what was
212 observed in female *O. fasciatus* (Amukamara et al. 2020) in which knockdown of *Dnmt1*
213 expression prior to the stage of oocyte development inhibited all oocyte formation. One
214 interpretation of this result is that *Dnmt1* is required for successful progression through meiosis.
215 However, it is clear that reducing *Dnmt1* expression had an impact beyond simply reducing the
216 ability to enter or complete meiosis. A block to progression through meiosis, as demonstrated by
217 the *Boule* knockdown, spermatogonia and primary spermatocytes would continue to be born but

218 remain viable after a failure to complete meiosis. In the *Dnmt1* knockdowns, however, there
219 were fewer germ cells of any type, and those that remained in the testis tubule often appeared to
220 have abnormal and condensed nuclei. It remains to be determined if *Dnmt1* is required for
221 meiosis or if the association with meiosis is a correlation; *Dnmt1* could be required for viability
222 of germ cells and act at the stage of development at which they would be undergoing meiosis.

223 Previous studies on the function of *Dnmt1* in insect spermatogenesis have not documented any
224 effect on male fertility. Knockdown of *Dnmt1* in the red flour beetle, *T. castaneum* (Schulz et al.
225 2018) had no effect on the fecundity of female mating partners was measured in the first nine
226 days post mating and the authors conclude that *Dnmt1* is not required for spermatogenesis in *T.*
227 *castaneum*. We suspect that the function of *Dnmt1* in spermatogenesis is not unique to *O.*
228 *fasciatus*, given the expression patterns of *Dnmt1* in other insects (Robinson et al. 2016, Kay et
229 al. 2018). In the *T. castaneum* study, the authors did not examine testis structure or design a
230 mating strategy that would exhaust the sperm stores of the males and so may have missed a
231 fertility effect. In holometabolous insects, including beetles, spermatocytes are typically formed
232 by the end of larval development (Economopoulos & Gordon 1971), thus males treated as pupae
233 would still emerge with large numbers of sperm in their testes. Here we showed that male *O.*
234 *fasciatus* treated with ds-*Dnmt1* RNA as sexually mature adults become sperm limited more
235 rapidly than control males. There is a potential alternative explanation, that *Dnmt1* knockdown
236 males could continue to produce sperm but that sperm was of low quality and unable to support
237 development. Given that the testes of ds-*Dnmt1* treated males were significantly smaller than
238 control males and had altered testis tubule structure, which indicated that spermatogenesis was
239 significantly impacted, we concluded that *Dnmt1* knockdown males are unable to replenish
240 sperm supplies. The functional role of *Dnmt1* in testes across other species remains to be tested.

241 **DNA methylation and germ cell development**

242 The knockdown of *Dnmt1* resulted in a reduction of DNA methylation within the testes, as
243 predicted. The effect was greater in the nymphs that were treated in an earlier stage of
244 development, as would be expected given the greater number of cell divisions that would occur
245 between treatment and collection of the testes between the 3rd and 5th instar treatments. The more
246 extreme phenotype in the 3rd instar treated males could be explained by the greater reduction in
247 methylated CpG. However, the percent methylation seen in the testes of the 5th instar ds-*Dnmt1*
248 treated males was similar to that seen in females treated at the 4th instar stage of development
249 (Amukamara et al. 2020), greater than a two-fold reduction in the percent methylated CpG
250 residues. In *Dnmt1* knockdown females, there was a compete loss of oocyte production when
251 DNA methylation was reduced to this level while in males the phenotype of the 5th instar *Dnmt1*
252 knockdowns was close to normal. This disconnect between reduction of DNA methylation and
253 phenotypic effects mirrors what has been seen in the beetle, *T. castaneum* (Schulz et al. 2018). In
254 this species, the reduction of DNA methylation is an evolved difference rather than an
255 experimental effect, but the results are similar to what we have observed in *O. fasciatus*; DNA
256 methylation is not required for function of somatic cells, but downregulation of *Dnmt1*
257 expression leads to specific germ cell effects. The lack of correlation between extent of
258 methylation and function in germ cells strengthens our hypothesis that there may be a pleiotropic
259 function for *Dnmt1* in germ cells that acts independently of DNA methylation levels.
260 Alternatively, DNA methylation may have a specific role in the germ cells that it does not play in
261 somatic cells. Perhaps DNA methylation is required for proper gene expression in germ cells or
262 it may be required for transposon silencing only in germ cells. However, demethylation of
263 ovarian tissue in *O. fasciatus* showed little relationship between methylation levels and gene

264 expression, with few differentially transcribed genes (Bewick et al. 2019). Another possibility is
265 that DNA methylation state may be a prerequisite for successful completion of meiosis and not
266 mitosis. For example, *O. fasciatus* has holocentric chromosomes and undergoes inverted meiosis
267 (Viera et al. 2009). During mitosis chromosomes have a kinetocore that extends across the
268 majority of the chromosome but in meiosis, the kinetochore plate is missing and microtubules
269 extend into the chromosome (Comings & Okada 1972). One could imagine that DNA
270 methylation might be required for this interaction. However, the complete lack of methylation
271 but a functional role of *Dnmt1* in *T. casteneum* oogenesis alongside our results argues for a
272 pleiotropic function for *Dnmt1* in gametogenesis that is independent of its role in DNA
273 methylation.

274 Conclusion

275 *Dnmt1* expression is required for germ cell development in both male and female *O. fasciatus*.
276 The block to germ cell development in *Dnmt1* knockdowns appeared to be associated with
277 meiosis, although it was not a simple block to progression through meiosis as germ cells are lost
278 from the testes. Thus, *Dnmt1* may be required for germ cell viability. It still remains to be
279 determined if the block in gametogenesis depends on DNA methylation or an alternative
280 function of *Dnmt1*, as suggested by the requirement for *Dnmt1* during gametogenesis in an insect
281 with a non-methylated genome (Schultz et al. 2018). Whatever the specific function of *Dnmt1* in
282 gametogenesis, the requirement for this enzyme in such a critical fitness function as the
283 production of gametes in representatives of different groups of insects raises important questions
284 as to how this enzyme and the entire methylation toolkit has evolved across the insect tree of life
285 (Lyko et al 2018, Provataris et al. 2018). Functional analysis of *Dnmt1* in the insect groups
286 where it is found, and study of how these functions are replaced in the species where it is no

287 longer found, will be essential for understanding the evolution of this important base
288 modification.

289 **Materials and Methods**

290 **Animal care**

291 All experimental animals were from colonies of laboratory reared *O. fasciatus* (Carolina
292 Biologicals, Burlington, NC) and were reared under standard rearing conditions of 12 hr:12 hr
293 light/dark at 27° C. To collect animals of known age and social conditions, eggs were removed
294 from the mass colonies and allowed to hatch in plastic storage containers containing *ad libitum*
295 deionized water and organic, raw sunflower seeds. For the nymph injections, nymphs were
296 pulled from mixed sex nymph colonies at the 3rd instar or 5th instar. For adult injections, nymphs
297 were separated by sex at the 4th instar and housed in single sex colonies. These were checked
298 daily and newly emerged adults. All experimental animals were placed into individual petri
299 dishes with food and water.

300 **Developmental expression**

301 Given our hypothesis that *Dnmt1* is required for development of germ cells and meiosis we
302 examined the expression levels of *Dnmt1* across testis development in males. Groups of nymphs
303 were staged and sexed. Testes were dissected from 4th and 5th instar nymphs and flash frozen in
304 liquid nitrogen and stored at -80° C. We also collected testes from virgin males on the day of
305 adult emergence and after sexual maturation at 7 days post-adult-emergence. We also collected
306 head, gut, and muscle samples from the sexually mature adult male individuals for tissue specific
307 expression.

308 Total RNA was extracted using a Qiagen RNA easy kit with Qiazol (Qiagen, Venlo, The
309 Netherlands) and complementary DNA (cDNA) synthesized from 500 ng RNA with aScript
310 cDNA Super-Mix (Quanta Biosciences, Gaithersburg, MD). Quantitative real-time PCR (qRT-
311 PCR) was used to determine expression levels of *Dnmt1* and two genes with known functions in
312 spermatogenesis, *Boule* and *Vasa*. Primers are described in Amukamara et al. 2020. As in
313 Amukamara et al. 2020, actin and GAPDH were used as reference genes. We have previously
314 validated these reference genes and they are accepted as robust reference genes in *O. fasciatus*
315 (Meinzer et al. 2019). We used a Roche LightCycler 480 with the SYBR Green Master Mix
316 (Roche Applied Science Indianapolis, IN). All samples were run with 3 technical replicates using
317 10 μL reactions. There were 10 biological replicates for each stage. Each biological replicate of
318 2nd, $3^{rd,}$ 4th, and 5th instar nymphs consisted of pools of 10, 5, 4, and 3 individuals, respectively.
319 Adult replicates consisted of individual animals. Sample size was based on past experience
320 balanced by the cost of qRT-PCR. Primer efficiency calculations, genomic contamination
321 testing, and endogenous control gene selection were performed as described in Cunningham et
322 al. 2014. We used the ΔΔCT method to compare levels of gene expression across the samples
323 (Livak and Schmittgen 2001). Gene expression was standardized per individual to account for
324 different numbers of individuals within each group at each developmental stage. Differences in
325 expression levels were analyzed using ANOVA in JMP Pro v14. If there was a significant
326 overall effect, we compared means using Tukey-Kramer HSD.

327 **RNAi preparation**

328 Double-stranded RNAs were prepared as described in Amukamara et al. 2020. Briefly, DNA
329 templates were prepared by PCR using gene-specific primers (Amukamara et al. 2020). Sense
330 and anti-sense RNA were transcribed together with an Ambion MEGAscript kit (ThermoFisher

331 Sci, Waltham, MA) and allowed to anneal to form a 404 bp ds-*Dnmt1* RNA. The concentration
332 of dsRNA was adjusted to 3 µg/µL in injection buffer (5 mM KCl, 0.1 mM NaH_2PO_4).

333 **Nymph injections, testis size and morphology**

334 To examine the effect of *Dnmt1* knockdown prior to or following the wave of meiosis initiated in
335 the 4th instar stage, nymphs were injected with ds-*Dnmt1* or control ds-RED injections at either
336 the 3rd instar or 5th instar stage of development. For further information on controls and testing
337 for potential off-target effects please see Amukamara et al. 2020. Nymphs were anaesthetized at
338 4° C for 20 minutes prior to injection. Nymphs were injected in the abdomen using pulled glass
339 capillary needles (Sutter Instrument Company micropipette puller model P-97, Novato, CA)
340 between the third and fourth abdominal segments (Chesebro et al. 2009). Nymphs were injected
341 with 2 µL volume for all injections. Following injections, nymphs were placed in individual petri
342 dishes and monitored for development. Date of adult emergence was recorded. We did not do a
343 power analysis, but based on preliminary data on the strength of the effect we aimed for 25
344 individual males for each treatment. Males were randomly assigned to a treatment group. Not all
345 males survived to age of dissection, resulting in final sample sizes of 22 and 19 for 3rd instar
346 males injected with buffer and ds-*Dnmt1*, respectively and 25 and 20 for 5th instar males injected
347 with buffer and ds-*Dnmt1*, respectively.

348 *Testis size*: At 7 to 10 days post-adult emergence, virgin males were dissected and their testes
349 were removed. Whole testes were allowed to settle into 1 mL Phosphate Buffered Saline (PBS)
350 and were imaged with a Leica M60 Stereomicroscope with Leica Application Suite software
351 (LAS v4). Testis area was measured on one of the pair from each male with the LAS by
352 outlining the whole testis with all 7 testis tubules. Differences in testis area were analyzed using
353 ANOVA in JMP Pro v14.

354 *Testis tubule structure*: *O. fasciatus* testes contain 7 individual testis tubules surrounded by a
355 relatively impermeable, autofluorescent membrane. Individual testis tubules were removed from
356 the outer membranous sheath for fixation and staining. Males from each treatment were dissected
357 across 4 dissection days. Testis tubules from individual males within a treatment were pooled for
358 staining. Thus each day one tube was a replicate with tubules from several individual males.
359 Tubules were fixed for 30 minutes in 4% formaldehyde in PBS plus 0.1% Triton-X100 (PBT)
360 and stained for evidence of cell division using an α-phosphohistone H3 Ser10 (pHH3) primary
361 antibody (Millipore antibody 06-570, Sigma-Aldrich, St. Louis, MO). α-phosphohistone H3
362 (pHH3) stains for chromosome condensation in preparation for mitosis and meiosis (Hans &
363 Dimitrov 2001, Prigent & Dimitrov 2003). The secondary antibody was an Alexa Fluor goat-
364 anti-rabbit 647 (ThermoFisher Scientific, Waltham, MA). Following antibody staining the
365 tubules were stained with DAPI (0.5 μg/mL PBT) to visualize nucleic acids. Stained tubules
366 were mounted in Mowiol 4-88 mounting medium (Sigma-Aldrich, St. Louis, MO) and visualized
367 with an Olympus BX51 Fluorescent microscope. Images were taken of every testis tubules
368 present on each slide. Representative images are presented in the figures.

369 **Quantitative Real Time PCR**

370 While we had evidence that all our RNAi treatments successfully knocked down expression in
371 females (Amukamara et al. 2020), to confirm that our RNAi treatment was effective in males,
372 total RNA and genomic DNA was extracted from flash frozen testes of a subsample of males 6
373 to 10 days following injection with the dsRNA using a Qiagen Allprep DNA/RNA Mini Kit
374 (Qiagen, Venlo, The Netherlands). Expression levels for *Dnmt1* was analyzed using qRT-PCR as
375 described above.

376 **Quantification of DNA methylation**

377 The DNA from each prep used for qRT-PCR was used to prepare MethylC-seq libraries as
378 described in Urich et al. 2015 and Amukamara et al. 2020. Samples were sequenced on a
379 NextSeq500 and qualified reads were aligned to the *O. fasciatus* genome assembly according to
380 previously published methods (Schmitz et al. 2013). The percent DNA methylation was
381 calculated by dividing the total number of methylated CpG sites by the total number of CpG sites
382 (Schultz et al. 2012). Spiked in Lambda DNA, which is fully demethylated, was used as a control
383 for the sodium bisulfite conversion rate of unmodified cytosines. Three individuals were
384 sequenced for each treatment.

385 **Adult injections**

386 *RNAi treatment*: Sexually mature virgin males (7 days post-adult-emergence) were injected with
387 3 µL ds-*Dnmt1* RNA or control injections using a pulled glass capillary needle between the third
388 and fourth abdominal segments (Chesebro et al. 2009). Control injections for the male fecundity
389 experiments were injection buffer alone. We used ds-RED control injections for the testis
390 imaging experiment. Previous studies from our lab have shown no difference in buffer alone
391 controls or non-specific ds-RNA (Bewick et al. 2019). Following injection males were placed
392 into individual petri dishes and provided with *ad libitum* food and water. We did not do a power
393 analysis, but based on preliminary data on the strength of the effect we aimed for 30 individual
394 males for each treatment. Males were randomly assigned to a treatment group.

395 *Male fecundity*: Preliminary experiments had shown that two previous matings were required to
396 deplete sperm stores. Therefore, in order to allow males to deplete sperm stores acquired during
397 nymphal development and sexual maturation, males were placed in mating trials with three 7- to
398 10-day-old virgin females, one provided each week. The first female was placed in the male's
399 petri on the day of injection with cotton wool as an oviposition substrate. The female and all eggs

400 were removed at the end of the week (7 days post-injection) and discarded and replaced with a
401 second 7- to 10-day-old virgin female and fresh cotton wool. Again, at the end of the week (14
402 days post-injection), the female and all resulting eggs were discarded. A third, focal, 7- to 10-
403 day-old virgin female was placed with the male with fresh cotton wool. The 3rd female and
404 experimental male were given one week to mate before the male was removed from the petri
405 dish for analysis of testis size and structure. The female was maintained for her lifetime,
406 provided with *ad libitum* food and water. The eggs produced by the 3rd female were collected
407 from the petri dish twice a week at 3-4 day intervals and the oviposition substrate replaced with
408 fresh cotton wool. The eggs collected were placed in a separate container and allowed to develop
409 to hatching (approximately 7-10 days following collection) and then frozen at -20° C until
410 assayed. We recorded the first collection date for which no eggs hatched. We analyzed the time
411 to end of fertilized eggs due to sperm depletion relative to treatment using a survival analysis
412 (Wilcoxon Rank Sum test) using JMP Pro v14.1. Not all males survived to date of dissection, or
413 their mates died during the course of egg collection, requiring these males to be removed from
414 the analysis, resulting in a sample size of 21 control and 20 ds-*Dnmt1* treated males in the final
415 fecundity analysis.

416 *Testis size*: At the end of the one-week mating trial with the 3rd female (21 days post-injection),
417 males were dissected and their testes removed into 1 mL Phosphate Buffered Saline (PBS).
418 Whole testes were photographed and measured as described above. Not all males survived to
419 date of dissection, resulting in a final sample size of 28 control and 25 ds-*Dnmt1* treated males.

420 *Testis tubule structure*: Testis tubules from mated males were isolated, fixed and stained as
421 described above.

422 **Acknowledgments**

The authors acknowledge Allen J. Moore and other members of the Moore lab for many helpful discussions. We acknowledge Luvika Gupta, who's undergraduate research provided preliminary data used in our experimental design. We also would like to acknowledge Tyler Earp for preparing and analyzing low throughput whole genome bisulfite sequencing data.

Competing Interests

The authors have no competing interests in regards to this work.

430 **References**

431 Amukamara A.U., J. T. Washington, Z. Sanchez, E.C. McKinney, A. J. Moore, R. J.
432 Schmitz, P. J. Moore. More than DNA methylation: does pleiotropy drive the complex
433 pattern of evolution of Dnmt1? *Frontiers in Ecology and Evolution* 8, 4 (2020).

434 Bewick, A.J., K. J. Vogel, A. J. Moore, R. J. Schmitz. Evolution of DNA methylation across
435 insects. *Molecular Biology and Evolution* 34, 654-66 (2016).

436 Bewick, A.J., Z. Sanchez, E. C. Mckinney, A. J. Moore, P. J. Moore, R. J. Schmitz. *Dnmt1* is
437 essential for egg production and embryo viability in the large milkweed bug,
438 *Oncopeltus fasciatus*. *Epigenetics & Chromatin* 12, 6 (2019).

439 Chesebro, J., S. Hrycaj, N. Mahfooz, A. Popadić. Diverging functions of Scr between
440 embryonic and post-embryonic development in a hemimetabolous insect, *Oncopeltus*
441 *fasciatus*. *Developmental Biology* 329, 142-151 (2009).

442 Comings, D.E., T. A. Okada. Holocentric chromosomes in *Oncopeltus*: kinetochore plates
443 are present in mitosis but absent in meiosis. *Chromosoma* 37, 177-192 (1972).
444 https://doi.org/10.1007/BF00284937

445 Cunningham, C.B., L. Ji, R. A. W. Wiberg, J. Shelton, E. C. McKinney, D. J. Parker, R. B.
446 Meagher, K. M. Benowitz, E. M. Roy-Zokan, M. G. Ritchie, S. J. Brown, R. J.
447 Schmitz, A. J. Moore. The genome and methylome of a beetle with complex social
448 behavior, *Nicrophorus vespilloides* (Coleoptera: Silphidae). *Genome Biology and*
449 *Evolution* 7, 3383-3396 (2015).

450 Dallai, R. Overview on spermatogenesis and sperm structure of Hexapoda. *Arthropod*
451 *Structure & Development* 43, 257-290 (2014). https://doi.org/10.1093/gbe/evy066

452 Eberhart, C.G., J. Z. Maines, S. A. Wasserman. Meiotic cell cycle requirement for a fly
453 homologue of human Deleted in Azoospermia. *Nature* 381, 783-785 (1996).

454 Economopoulos, A.P. H. T. Gordon. Growth and differentiation of the testes in the large
455 milkweed bug, *Oncopeltus fasciatus* (Dallas). *Journal of Experimental Zoology* 177,
456 391-405 (1971).

457 Ewen-Campen, B., T. E. Jones, C. G. Extavour. Evidence against a germ plasm in the
458 milkweed bug *Oncopeltus fasciatus*, a hemimetabolous insect. *Biology Open* 2, 556-
459 568 (2013).

460 Gegner, J., T.Gegner, H. Vogel, A. Vilcinskas. Silencing of the DNA methyltransferase 1
461 associated protein 1 (DMAP1) gene in the invasive ladybird *Harmonia axyridis* implies
462 a role of the DNA methyltransferase 1-DMAP1 complex in female fecundity. *Insect*
463 *Molecular Biology* 29, 148-159 (2020). https://doi.org/10.1111/imb.12616

464 Glastad, K.M., B. G. Hunt, M. A. Goodisman. Epigenetics in insects: genome regulation and
465 the generation of phenotypic diversity. *Annual Review of Entomology* 64, 185-203
466 (2019). doi.org/10.1146/annurev-ento-011118-111914

467 Hans, F., S. Dimitrov. Histone H3 phosphorylation and cell division. *Oncogene* 20, 3021-
468 3027 (2001).

469 Kay. S., D. Skowronski, B. G. Hunt. Developmental DNA methyltransferase expression in
470 the fire ant Solenopsis invicta. Insect Science 25, 57-65 (2018).

471 Lewis S.H., L. Ross, S. A. Bain, E. Pahita, S. A. Smith, R. Cordaux, et al. Widespread
472 conservation and lineage-specific diversification of genome-wide DNA methylation
473 patterns across arthropods. *PLoS Genetics* 16, e1008864 (2020).
474 https://doi.org/10.1371/journal.pgen.1008864

475 Livak, K.J., T. D. Schmittgen. Analysis of relative gene expression data using real-time
476 quantitative PCR and the 2− ΔΔCT method. *Methods* 25, 402-408 (2001).

477 Lyko, F. The DNA methyltransferase family: a versatile toolkit for epigenetic regulation.
478 *Nature Reviews Genetics* 19, 81-92 (2018).

479 Medrano, J.V., C. Ramathal, H. N. Nguyen, C. Simon, R. A. Reijo Pera. Divergent RNA-
480 binding proteins, DAZL and VASA, induce meiotic progression in human germ cells
481 derived in vitro. *Stem cells* 30, 441-451 (2012).

482 Meinzer, F., S. Dobler, A. Donath, J. N. Lohr. Robust reference gene design and validation
483 for expression studies in the large milkweed bug, *Oncopeltus fasciatus*, upon cardiac
484 glycoside stress. *Gene* 710, 66-75 (2019).

485 Prigent, C. S. Dimitrov. Phosphorylation of serine 10 in histone H3, what for?. *Journal of*
486 *Cell Science* 116, 3677-3685 (2003).

487 Provataris, P., K. Meusemann, O. Niehuis, S. Grath, B. Misof. Signatures of DNA
488 methylation across insects suggest reduced DNA methylation levels in holometabolan.
489 *Genome Biology and Evolution* 10, 1185-1197 (2018).

490 Robinson, K.L., D. Tohidi-Esfahani, F. Ponton, S. J. Simpson, G. A. Sword, N. Lo.
491 Alternative migratory locust phenotypes are associated with differences in the
492 expression of genes encoding the methylation machinery. *Insect Molecular Biology* 25,
493 105-115 (2016).

494 Schmidt, E. D., E. Sehn, A. Dorn. Differentiation and ultrastructure of the spermatogonial
495 cyst cells in the milkweed bug, *Oncopeltus fasciatus*. *Invertebrate Reproduction &*
496 *Development* 42, 163-178 (2002). DOI:10.1080/07924259.2002.9652773

497 Schmitz, R. J., Z. A. Lewis, M. G. Goll. DNA methylation: shared and divergent features
498 across eukaryotes. *Trends in Genetics* 35, 818-827 (2019).
499 doi.org/10.1016/j.tig.2019.07.007

500 Schmitz, R.J., Y. He, O. Valdés-López, S. M. Khan, T. Joshi, M. A. Urich, J. R. Nery, B.
501 Diers, D. Xu, G. Stacey, J. R. Ecker. Epigenome-wide inheritance of cytosine
502 methylation variants in a recombinant inbred population. *Genome Research* 23, 1663-
503 1674 (2013).

504 Schultz, M.D., R. J. Schmitz, J. R. Ecker. 'Leveling' the playing field for analyses of single-
505 base resolution DNA methylomes. *Trends in Genetics* 28, 583-585 (2012).
506 DOI:https://doi.org/10.1016/j.tig.2012.10.012

507 Schulz, N.K., C. I. Wagner, J. Ebeling, G. Raddatz, M. F. Diddens-de Buhr, F. Lyko, J.
508 Kurtz. Dnmt1 has an essential function despite the absence of CpG DNA methylation

509 in the red flour beetle *Tribolium castaneum*. *Scientific Reports* 8, 1-10 (2018).
510 https://doi.org/10.1038/s41598-018-34701-3

511 Shah, C., M. J. VanGompel, V. Naeem, Y. Chen, T. Lee, N. Angeloni, Y. Wang, Y. E. Y.
512 Xu. Widespread presence of human BOULE homologs among animals and
513 conservation of their ancient reproductive function. *PLoS Genetics* 6, e1001022 (2010).
514 doi.org/10.1371/journal.pgen.1001022

515 Tanaka, S.S., Y. Toyooka, R. Akasu, Y. Katoh-Fukui, Y. Nakahara, R. Suzuki, M.
516 Yokoyama, T. Noce. The mouse homolog of Drosophila Vasa is required for the
517 development of male germ cells. *Genes & Development* 14, 841-853 (2000).

518 Ulrich, M. S., J. R. Nery, R. Lister, R. J. Schmitz, J. R. Ecker. MethylC-seq library
519 preparation for base-resolution whole-genome bisulfite sequencing. *Nature Protocols*
520 10, 475–483 (2015). doi: 10.1038/nprot.2014.114

521 Viera, A., J. Page, J. Rufas. Inverted meiosis: the true bugs as a model to study. In:
522 Benavente, R., Volff J.-N. (eds): Meiosis. Genome Dynamics, Basel, Karger, 2009, vol
523 5, pp 137-156 (2009). https://doi.org/10.1159/000166639

524 Yajima, M., G. M. Wessel. The multiple hats of Vasa: its functions in the germline and in
525 cell cycle progression. *Molecular reproduction and development* 78, 861-867 (2011)

526 Zemach, A., I. E. McDaniel, P. Silva, D. Zilberman. Genome-wide evolutionary analysis of
527 eukaryotic DNA methylation. *Science* 328, 916-919 (2010).

528 Zhang, J. Y. Xing, Y. Li, C. Yin, C. Ge, F. Li. DNA methyltransferases have an essential role
529 in female fecundity in brown planthopper, Nilaparvata lugens. Biochemical and
530 Biophysical Research Communications 464, 83-88 (2015).

531 Zwier, M. V., E. C. Verhulst, R. D. Zwahlen, L. W. Beukeboom, L. van de Zande. DNA
532 methylation plays a crucial role during early Nasonia development. *Insect Molecular*
533 *Biology* 21, 129-138 (2012).
534

535 **Figure Legends**

536 **Figure 1.** Progression of spermatogenesis in *O. fasciatus*. In *O. fasciatus* spermatogenesis
537 progresses from the tip of the testis tubule. (A) Dapi-stained testis tubule of stock male. (B)
538 Diagram of the stages of spermatogenesis. At the apical tip (region I) of each of the seven testis
539 tubules there is a "rosette" of niche cells (blue) surrounded by the germline stem cells (B, green;
540 Schmidt et al. 2002). The rosette is not typically visible in confocal images of testis tubules and
541 markers for the rosette have not been identified yet. As spermatogonia (B, light gray) arise from
542 division of the germline stem cells, they are enclosed by cyst cells (B, yellow). In region II,
543 spermatogonia undergo mitotic transit amplification divisions to form spermatocysts containing
544 64 spermatogonia (Economopoulos & Gordon 1971, Ewen-Campen et al. 2013). Spermatocytes
545 (B, dark gray) in region III divide meiotically. *Oncopeltus fasciatus* undergoes inverted meiosis
546 (Viera et al. 2009). Primary spermatocytes undergo the first meiotic division to produce diploid
547 secondary spermatocytes. The meiotic division of the secondary spermatocytes produce the
548 haploid spermatids (B, dark blue) in region IV that then differentiate into spermatozoa in the
549 region V at the terminal end of the testis tubule.

550 **Figure 2**. Expression pattern of *Dnmt1* within the developing testes mirrored that the two
551 gametogenesis genes *Boule* and *Vasa*. *Dnmt1* expression (A) was highest in the larval stages
552 where spermatogenesis is initiated compared to the testes of newly emerged (day 0) and virgin
553 sexually mature (day 7-10) adults. This is similar to the expression patterns of *Boule* (B), in
554 which expression was higher in the 4th and 5th larval stages during which the transition to meiosis
555 occurs compared to newly emerged and virgin sexually mature adults. Expression of *Vasa* (C)
556 demonstrated a similar pattern, with the highest expression in the 4th instar stage and lowest in
557 sexually mature virgin males. Black dots and bars represent mean and SE. Grey dots represent

558 data points for each individual tested. Lower case letters designate significant differences ($p <$
559 0.05) among pairwise comparisons using *post-hoc* Tukey-Kramer HSD test.
560 **Figure 3.** Expression of *Dnmt1* was reduced in the testes of adult males treated with ds-*Dnmt1* at
561 both stages of development. Relative gene expression is standardized to expression levels in
562 control treatments. Black dots and bars represent mean and SE. Grey dots represent data points
563 for each individual tested.
564 **Figure 4.** Downregulation of *Dnmt1* during the 3rd instar stage of development significantly
565 reduced the size of the testis in sexually mature males. There was no effect of downregulation of
566 *Dnmt1* on testis size when treatment occurred during the 5th instar stage of development after
567 meiosis has been initiated. Black dots and bars represent mean and SE. Grey dots represent data
568 points for each individual tested.
569 **Figure 5**.
570 Timing of treatment during development determined the effect on testis structure of adults that
571 develop from *Dnmt1* (Panels B and D) knockdown males. In control testis tubules from males
572 injected with ds-RED (A and C), spermatogonia divided mitotically in region II to form
573 spermatocysts as is observed in untreated males. Mitotic spermatogonia are labeled with anti-
574 phosophohistone 3 antibodies in region II of the testis tubule (C, arrowhead). Meiotic divisions
575 also occured as in untreated males in ds-RED injected males. In our ds-RED control samples, a
576 band of synchronously dividing spermatocysts, identified by positive anti-phosphohistone H3
577 antibody staining, was present at the interface between primary and secondary spermatocytes (A,
578 C). In testes from males with *Dnmt1* knockdown in the 3rd instar (B), the anterior tip of the testis
579 tubule showed evidence of mitotic activity (arrowhead). However, there were fewer
580 spermatocytes present and the spermatocysts in this region were disorganized and there was little

581 evidence of the band of positive anti-phosphohistone H3 stained meiotic spermatocytes. The
582 testis tubule structure from males treated with ds-*Dnmt1* following meiosis at the 5th instar stage
583 of development (D) was more similar to the controls than those treated at the 3rd instar stage of
584 development. In ds-*Dnmt1* males treated at the 5th instar stage, there were positive anti-
585 phosphohistone H3 stained spermatogonia (arrowhead) and spermatocytes (arrow). There were
586 differences between males treated as 5th instars with ds-RED males and ds-*Dnmt1*, however,
587 including spermatocysts containing cells with highly condensed nuclei that were not present in
588 the controls and fewer spermatocysts containing spermatids or spermatozoa. All images taken at
589 10X magnification.
590 **Figure 6**. Females mated to control males lay fertilized eggs longer than females mated to
591 *Dnmt1* knockdown males. Eggs were collected twice per week and eggs allowed to develop to
592 hatching. Eggs that did not hatch showed no sign of development, indicating that they had not
593 been fertilized. Both treatments demonstrate a decrease in proportion of eggs that hatch over
594 time, but the ds-*Dnmt1* treatment group shows a faster decrease.
595 **Figure 7**. Testis structure breaks down in *Dnmt1* knockdown males treated as adults after having
596 sperm replenishment induced by mating activity. The regions of spermatogenesis were apparent
597 in mated males following 3 weeks of mating activity in control testis tubules (A and B) and the
598 evidence of both mitotic division in spermatogonia (B, arrowhead) and the band of meiotic
599 divisions was clear from anti-phosphohistone H3 staining. In *Dnmt1* knockdown males at low
600 magnification (C), the anterior tip of the testis tubule looked relatively normal. However, the
601 region containing both the primary and secondary spermatocytes was disorganized.
602 Spermatocyst structure was broken down, and the nuclei of the primary and secondary
603 spermatocytes had lost their characteristic structure (Ewen-Campen et al. 2013). Finally, there

604 were fewer mature spermatids in the posterior end of the testis tubule. At higher magnification
605 (D), it was apparent that nuclear structure in the anterior tip was also affected by the knockdown,
606 both in the spermatogonia and spermatocytes. Spermatogonia nuclei in the *Dnmt1* knockdown
607 testis tubules (D) were more condensed than in the control testis tubules (B), although they still
608 seemed to be organized into spermatocysts. Spermatocyte nuclei, however, were fewer in
609 number than in controls, did not have their characteristic shape (Ewen-Campen et al. 2013,
610 Economopoulos & Gordon 1971), and were not organized in spermatocytes. A and C:10X
611 magnification, B and D: 20X magnification.
612

613 Figure 1.

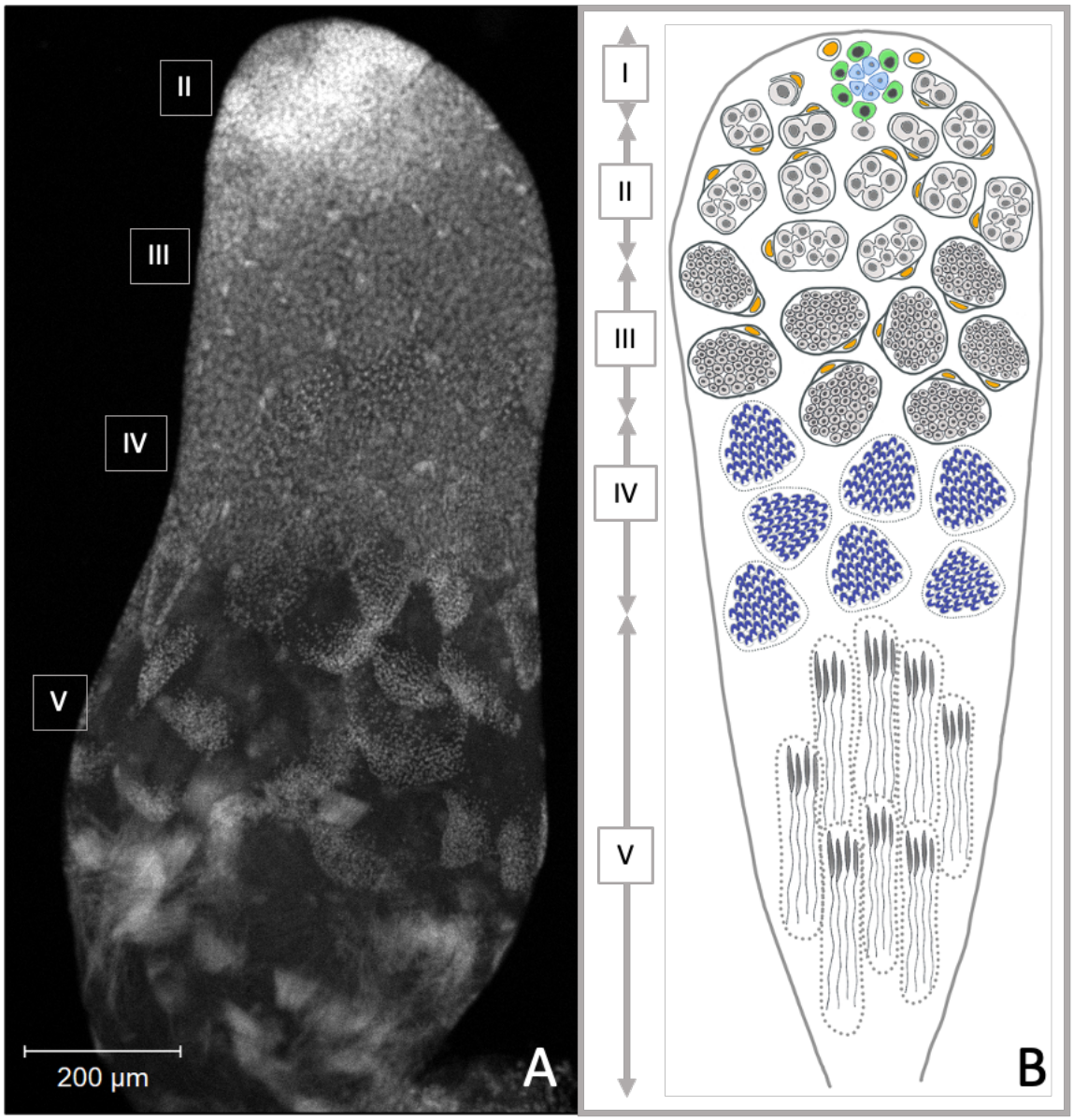

614

615

616 Figure 2.

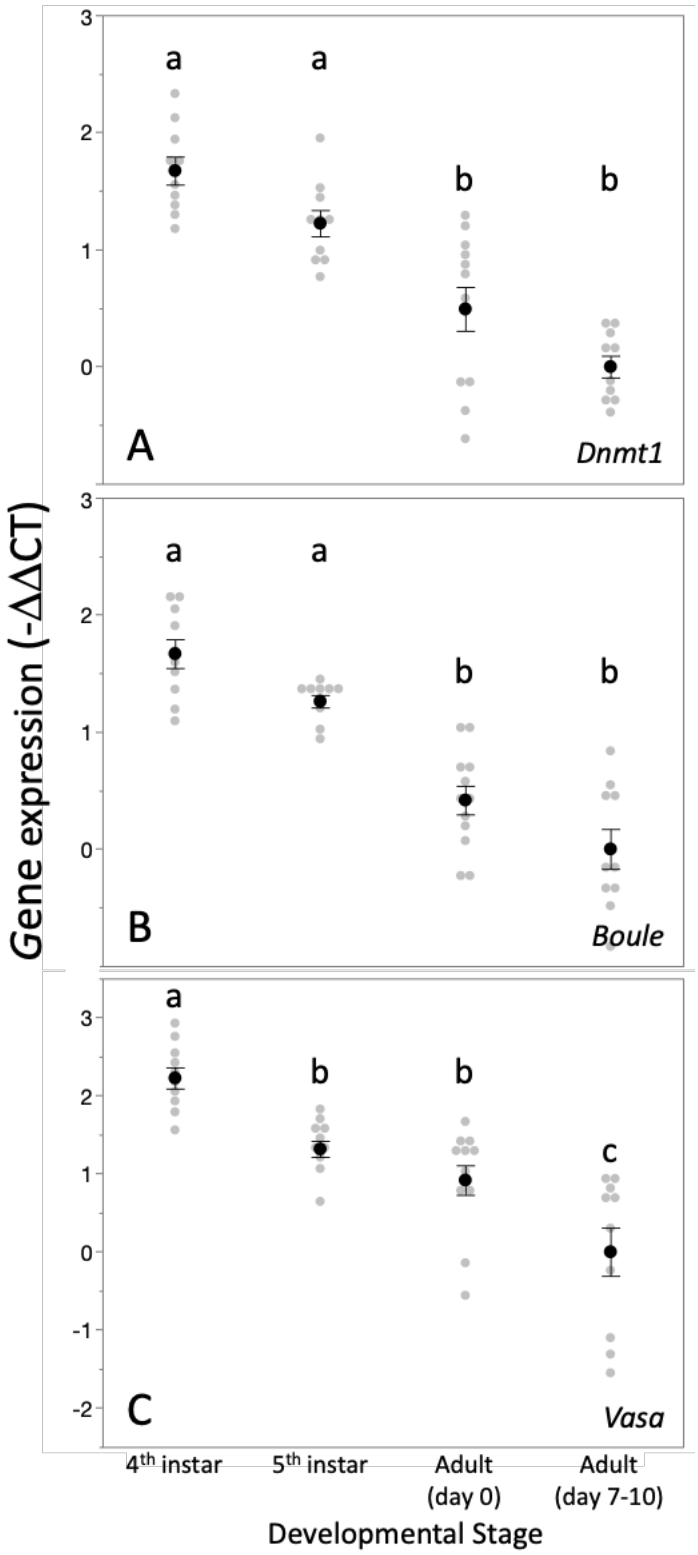

617

618

619 Figure 3

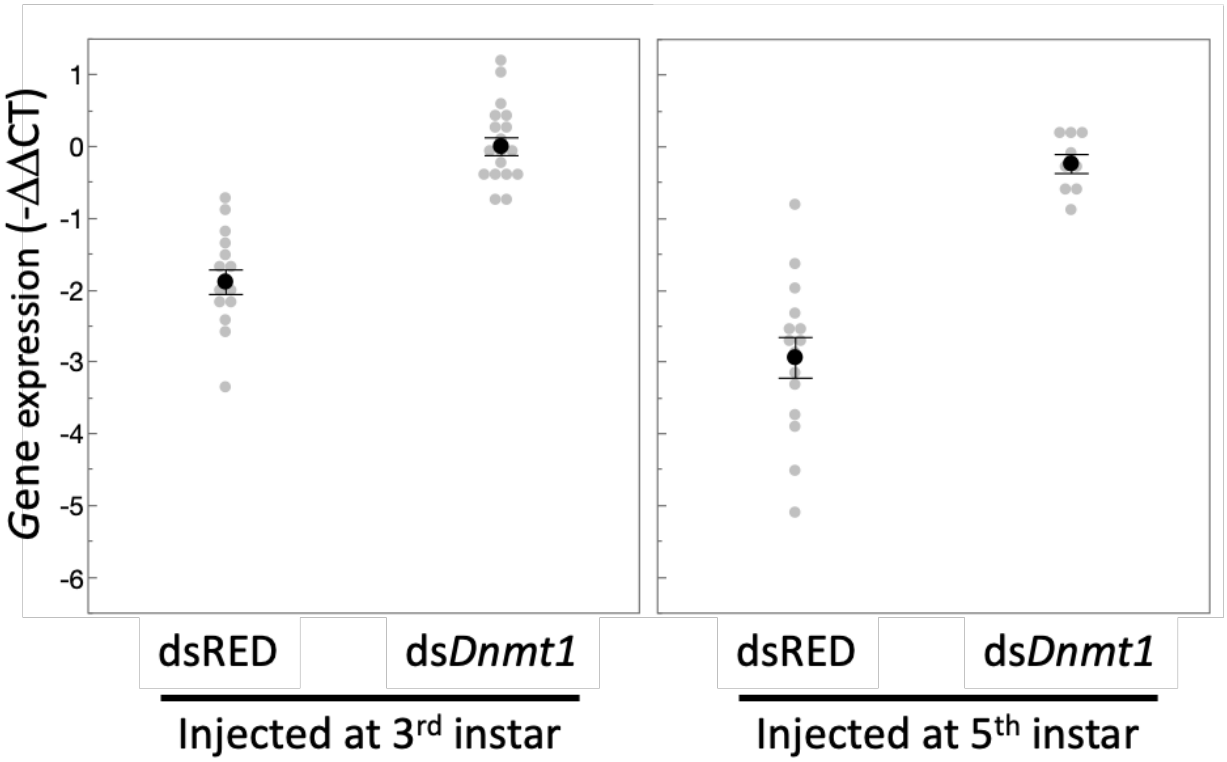

620

621

622 Figure 4.

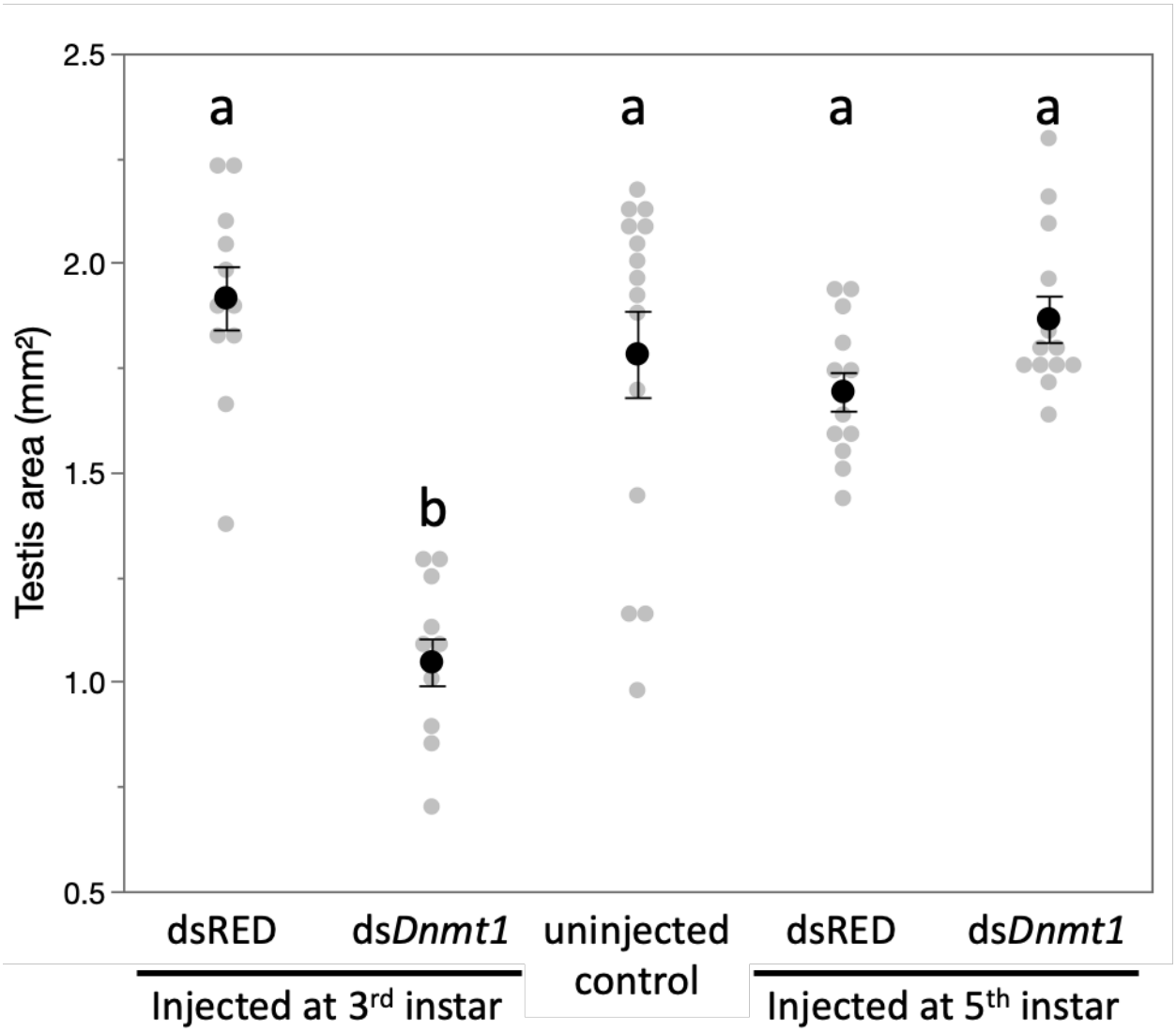

623

624

625 Figure 5.

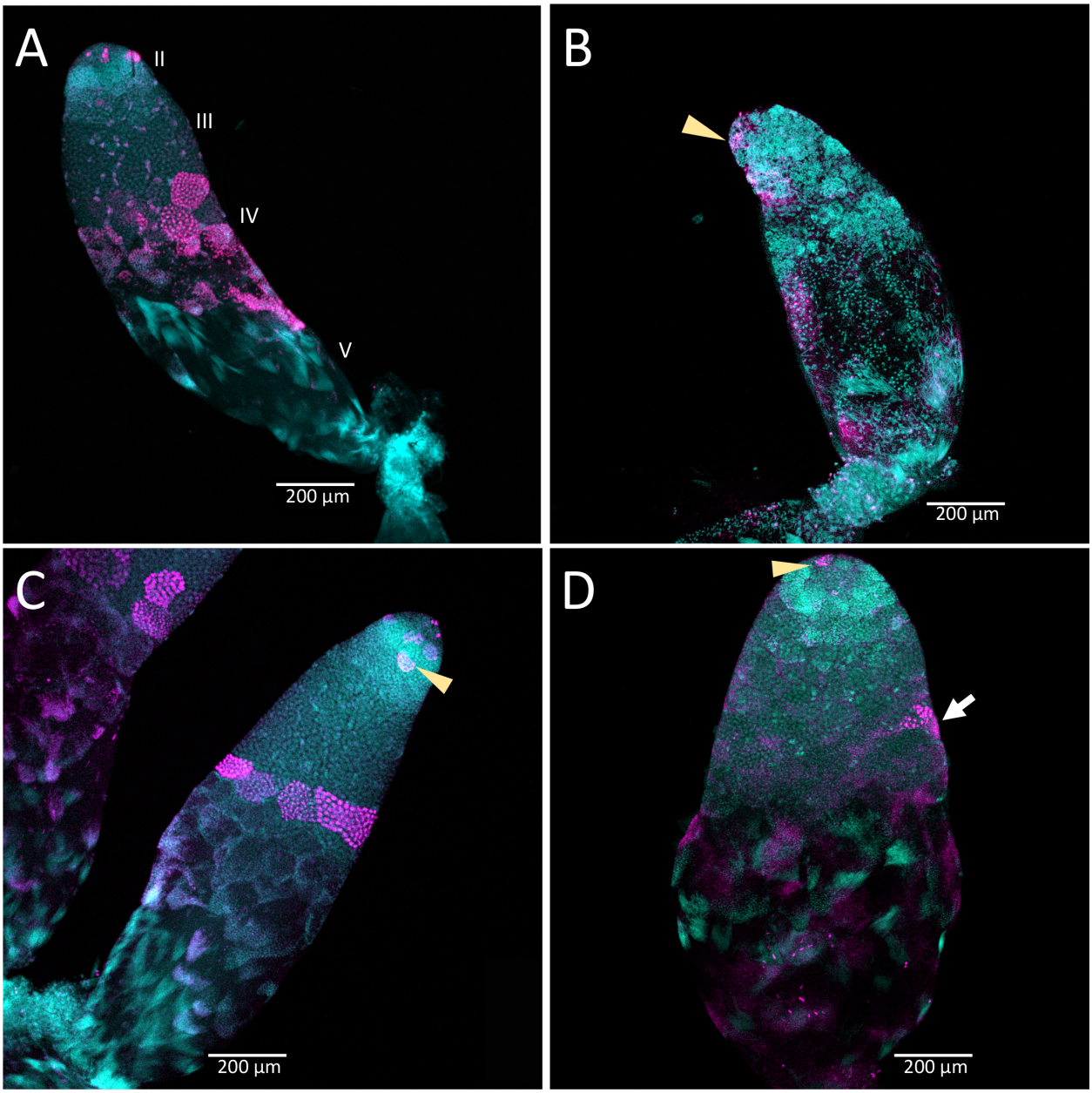

626

627 Figure 6.

628

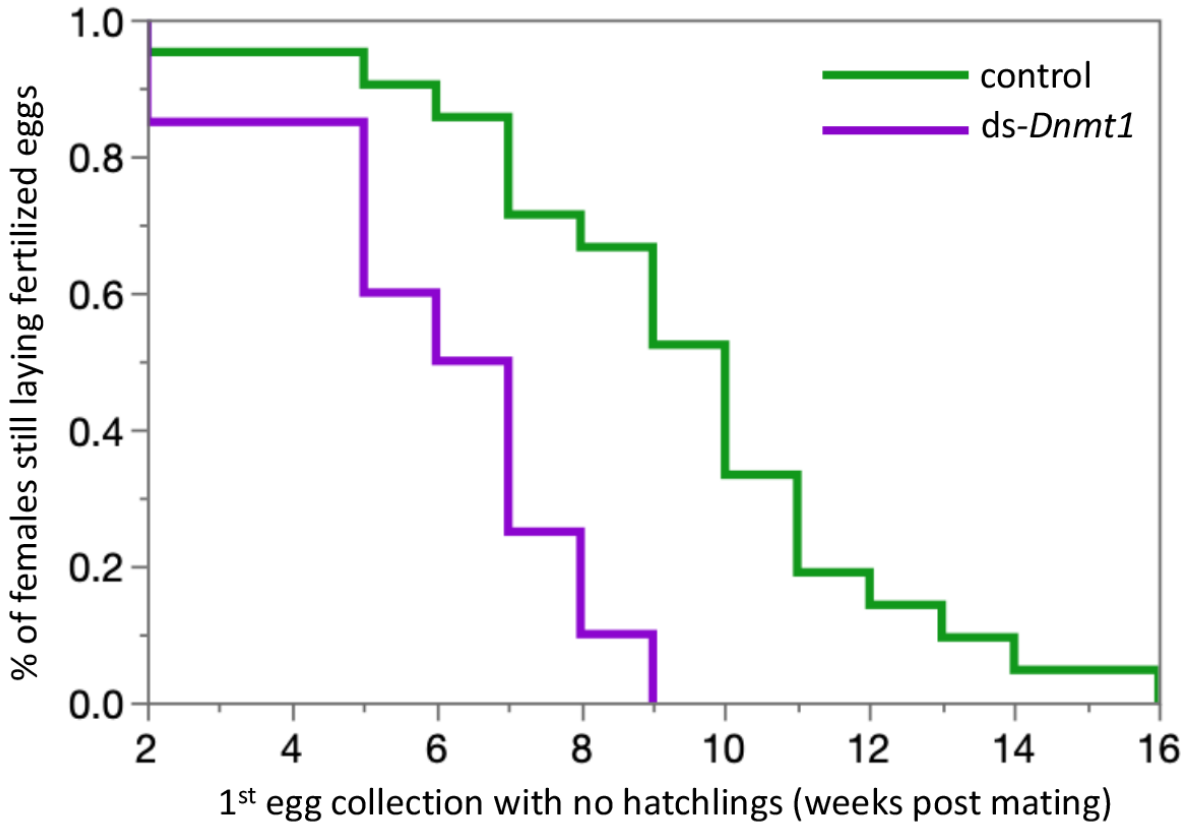

629

630

631 Figure 7.

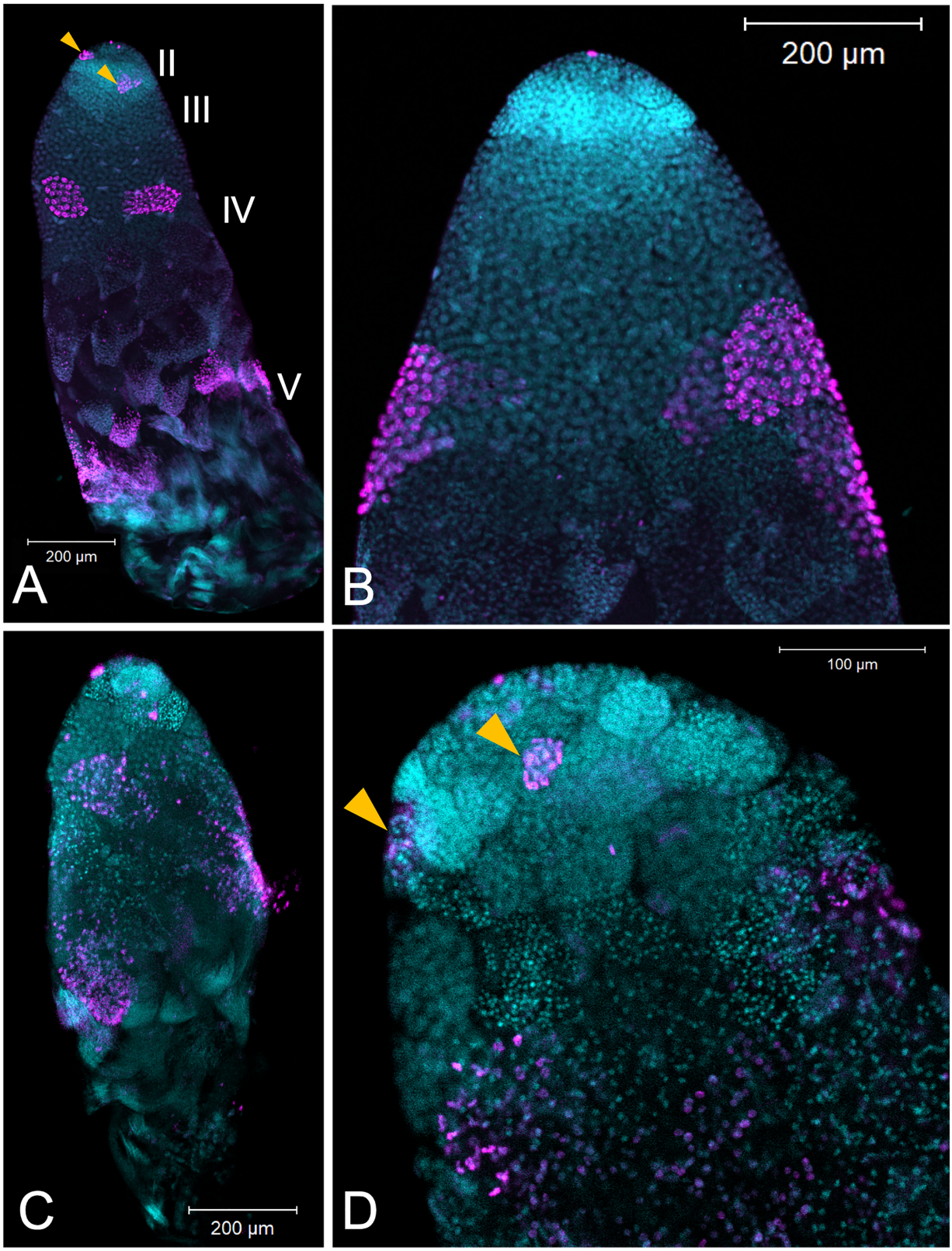

632